Cell Reports

Recruitment of Cytosolic J-Proteins by TOM Receptors Promotes Mitochondrial Protein Biogenesis

Graphical Abstract

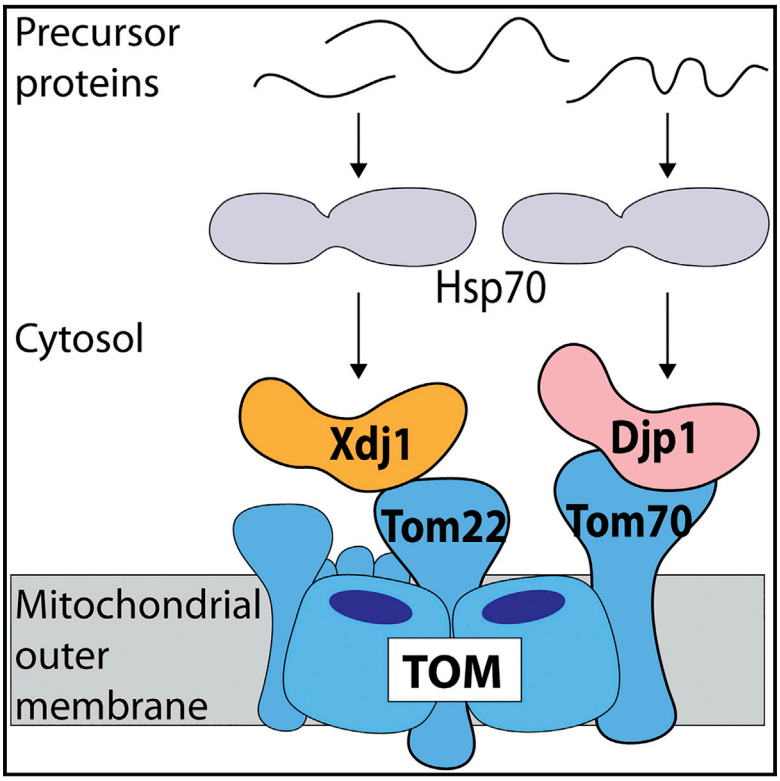

Highlights

- The receptor Tom22 recruits the cytosolic J-protein Xdj1 to mitochondria
- Xdj1 delivers preproteins to Tom22 and promotes biogenesis of the TOM complex
- The receptor Tom70 recruits a different cytosolic J-protein, Djp1
- Mitochondrial receptors selectively recognize cytosolic J-protein co-chaperones

Authors

Łukasz Opaliński, Jiyao Song, Chantal Priesnitz, ..., Bettina Warscheid, Nikolaus Pfanner, Thomas Becker

Correspondence

nikolaus.pfanner@biochemie.uni-freiburg.de (N.P.), thomas.becker@biochemie.uni-freiburg.de (T.B.)

In Brief

Opaliński et al. report that mitochondrial protein import receptors selectively recognize J-protein co-chaperones of the cytosol. The co-chaperones bind hydrophobic precursor proteins and assist in transferring them to the receptors of the mitochondrial protein entry gate.

Opaliński et al., 2018, Cell Reports *25*, 2036–2043
November 20, 2018
https://doi.org/10.1016/j.celrep.2018.10.083

CellPress

OPEN ACCESS
CellPress

Cell Reports
Report

Recruitment of Cytosolic J-Proteins by TOM Receptors Promotes Mitochondrial Protein Biogenesis

Łukasz Opaliński,[1,5] Jiyao Song,[1] Chantal Priesnitz,[1,2] Lena-Sophie Wenz,[1,6] Silke Oeljeklaus,[3,4] Bettina Warscheid,[3,4] Nikolaus Pfanner,[1,4,7,*] and Thomas Becker[1,4,*]

[1]Institute of Biochemistry and Molecular Biology, ZBMZ, Faculty of Medicine, University of Freiburg, 79104 Freiburg, Germany
[2]Faculty of Biology, University of Freiburg, 79104 Freiburg, Germany
[3]Institute of Biology II, Biochemistry and Functional Proteomics, Faculty of Biology, University of Freiburg, 79104 Freiburg, Germany
[4]BIOSS Centre for Biological Signalling Studies, University of Freiburg, 79104 Freiburg, Germany
[5]Present address: Faculty of Biotechnology, Department of Protein Engineering, University of Wroclaw, 50-383 Wroclaw, Poland
[6]Present address: Sanofi Deutschland GmbH, 65926 Frankfurt am Main, Germany
[7]Lead Contact
*Correspondence: nikolaus.pfanner@biochemie.uni-freiburg.de (N.P.), thomas.becker@biochemie.uni-freiburg.de (T.B.)
https://doi.org/10.1016/j.celrep.2018.10.083

SUMMARY

Mitochondria possess elaborate machineries for the import of proteins from the cytosol. Cytosolic factors like Hsp70 chaperones and their co-chaperones, the J-proteins, guide proteins to the mitochondrial surface. The translocase of the mitochondrial outer membrane (TOM) forms the entry gate for preproteins. How the proteins are delivered to mitochondrial preprotein receptors is poorly understood. We identify the cytosolic J-protein Xdj1 as a specific interaction partner of the central receptor Tom22. Tom22 recruits Xdj1 to the mitochondrial surface to promote import of preproteins and assembly of the TOM complex. Additionally, we find that the receptor Tom70 binds a different cytosolic J-protein, Djp1. Our findings suggest that cytosolic J-proteins target distinct TOM receptors and promote the biogenesis of mitochondrial proteins.

INTRODUCTION

The vast majority of mitochondrial proteins are synthesized as precursors on cytosolic ribosomes and imported by the translocase of the outer mitochondrial membrane (TOM). The initial receptors Tom20 and Tom70 and the central receptor Tom22 recognize incoming precursor proteins, and Tom40 forms a protein-conducting channel across the outer membrane (Endo and Yamano, 2010; Schleiff and Becker, 2011). Specialized protein machineries mediate further sorting of the precursor proteins toward the different mitochondrial subcompartments (Neupert and Herrmann, 2007; Endo and Yamano, 2010; Wiedemann and Pfanner, 2017).

Whereas the translocases of the mitochondrial membranes have been studied in detail, much less is known about the delivery of precursor proteins from cytosolic ribosomes to mitochondria. Evidence for a co-translational import mechanism has been reported for some precursor proteins (Williams et al., 2014), yet the majority of precursor proteins likely follow a post-translational import pathway (Neupert and Herrmann, 2007; Wiedemann and Pfanner, 2017). Cytosolic factors are needed to prevent the aggregation of preproteins and keep them in an import-competent state. Several cytosolic proteins have been described that guide precursor proteins to the mitochondrial surface (Young et al., 2003; Endo and Yamano, 2010; Papić et al., 2013; Sahi et al., 2013; Hoseini et al., 2016; Itakura et al., 2016; Hansen et al., 2018; Jores et al., 2018). It is largely unknown whether these factors play a general role in protecting newly synthesized proteins or whether they fulfill precursor-specific functions. Molecular chaperones like heat shock proteins of 70 kDa (Hsp70) and 90 kDa (Hsp90) are involved in protein transfer to organelles (Young et al., 2003; Endo and Yamano, 2010; Jores et al., 2018). These chaperones play crucial roles in various vital cellular processes, including protein folding, assembly of ribosomes, vesicle budding, intracellular protein transport, removal of aggregated and misfolded proteins, and signaling pathways (Walsh et al., 2004; Bukau et al., 2006; Kampinga and Craig, 2010). Hsp40 co-chaperones, also termed DnaJ-related proteins (J-proteins), can help in substrate transfer to Hsp70s and stimulate their ATPase activity (Walsh et al., 2004; Kampinga and Craig, 2010). The cytosol of yeast cells contains 13 different J-proteins that are involved in a remarkable diversity of cellular processes (Walsh et al., 2004; Sahi et al., 2013). The following J-proteins have been implicated in protein sorting to mitochondria. (1) Lack of the abundant cytosolic J-protein Ydj1 causes accumulation of mitochondrial precursor proteins (Atencio and Yaffe, 1992; Caplan et al., 1992; Becker et al., 1996). A double depletion of Ydj1 and Sis1 impairs the biogenesis of β-barrel proteins of the mitochondrial outer membrane (Jores et al., 2018). (2) Absence of Xdj1 shows a synthetic growth defect with the lack of Pam17 of the inner membrane presequence translocase-associated motor (PAM) (Sahi et al., 2013). (3) Loss of Djp1 affects import of Mim1 of the mitochondrial import (MIM) complex of the outer membrane (Papić et al., 2013). Djp1 binds the precursors of several hydrophobic mitochondrial proteins in the cytosol and at the surface of the endoplasmic reticulum and supports

their transfer to mitochondria (Hansen et al., 2018; Jores et al., 2018).

To date, a specific interaction has been reported for the mitochondrial protein import receptor Tom70 and cytosolic Hsp70/Hsp90 that promote the transfer of hydrophobic carrier proteins destined for the inner membrane (Young et al., 2003). Additional co-chaperones act together with Hsp70/Hsp90 in preprotein transfer, and an association of chaperone/co-chaperone complexes with Tom20 and Tom70 has been reported (Papić et al., 2013; Hoseini et al., 2016; Jores et al., 2018). Here, we identified Xdj1 as a specific binding partner of Tom22. Xdj1 is recruited to mitochondria by Tom22 to deliver precursors of outer and inner membrane proteins. In addition, Djp1 binds to Tom70 to facilitate protein import. Thus, cytosolic J-proteins are recruited by mitochondrial receptors to promote the biogenesis of hydrophobic proteins.

RESULTS

Xdj1 Binds to the Cytosolic Domain of Tom22

To identify proteins interacting with Tom22, we used a yeast strain expressing His-tagged Tom22 and stable isotope labeling by amino acids in cell culture (SILAC) (Ong et al., 2002). Wild-type cells were grown in the presence of heavy isotope-coded arginine and lysine, whereas $Tom22_{His}$ cells were grown in medium containing the corresponding light amino acids. Crude mitochondrial preparations consisting of mitochondria and associated cellular fractions (Morgenstern et al., 2017) were lysed with the non-ionic detergent digitonin and subjected to affinity purification, followed by quantitative mass spectrometry of purified $Tom22_{His}$ complexes. Potential interaction partners of Tom22 were determined based on the mean light-over-heavy protein abundance ratio across three biological replicates (Figure 1A; Table S1). Proteins co-purified with high enrichment factor ($\geq$100) included TOM subunits, the abundant metabolite channel Por1 that interacts with TOM (Müller et al., 2016), and one member of the cellular chaperone system, Xdj1 (Schwarz et al., 1994; Sahi et al., 2013).

Deletion of the *XDJ1* gene is not lethal for yeast cells (Schwarz et al., 1994; Sahi et al., 2013). *xdj1*Δ cells grew like wild-type cells on fermentable medium; however, their growth was impaired on non-fermentable medium at elevated temperature (Figure S1A), indicating that Xdj1 is required for optimal cell growth under conditions where an increased mitochondrial activity is needed.

Different views were reported about the subcellular localization of Xdj1. Studies on J-proteins described Xdj1 as a soluble protein of the cytosol (Walsh et al., 2004; Sahi et al., 2013), whereas high-throughput proteomic studies of mitochondrial fractions found Xdj1 in association with mitochondria (Zahedi et al., 2006; Morgenstern et al., 2017). We observed by fluorescence microscopy that Xdj1 carrying a GFP tag localized to both the cytosol and mitochondria (Figure 1B). Upon incubation of isolated mitochondria with proteinase K, Xdj1 was accessible to the protease like Tom22 that exposes its receptor domain toward the cytosol (Figure S1B). Taken together, Xdj1 shows a dual localization in the cytosol and at the mitochondrial surface.

We synthesized Xdj1 in a cell-free system and analyzed its interaction with the purified cytosolic domains of the receptors Tom20, Tom22, and Tom70 (Brix et al., 1997; Becker et al., 2011). Only the receptor domain of Tom22 specifically bound Xdj1, but not that of Tom20 or Tom70 (Figure 1C). We recombinantly expressed Xdj1 and additionally the cytosolic J-proteins Ydj1 and Djp1 (Caplan et al., 1992; Papić et al., 2013; Sahi et al., 2013; Jores et al., 2018) as glutathione S-transferase (GST) fusion proteins and analyzed their interaction with the cytosolic domain of Tom22. Xdj1, but neither Djp1 nor Ydj1, bound the Tom22 receptor domain (Figures 1D and S2A). These results demonstrate that Xdj1 directly interacts with the purified receptor domain of Tom22.

Distinct TOM Receptors Recruit Xdj1 and Djp1 to Mitochondria

To investigate whether Xdj1 binds to Tom22 present in the TOM complex or to unassembled Tom22, we incubated His-tagged Xdj1 with digitonin-lysed mitochondria, co-purified bound proteins, and analyzed them by blue native electrophoresis. $Xdj1_{His}$ bound to Tom22 present in the TOM complex (Figure 1E). As an independent assay, we used a yeast strain containing hemagglutinin (HA)-tagged Tom40 (Becker et al., 2011). ^{35}S-labeled Xdj1 was incubated with isolated mitochondria and co-purified via $Tom40_{HA}$ upon lysis of the mitochondria (Figure 1F), demonstrating an association of Xdj1 with the TOM complex.

Pretreatment of isolated mitochondria with protease to remove receptor domains exposed to the cytosol impaired the binding of Xdj1 to mitochondria (Figure S2B). *tom22*Δ mitochondria were impaired in binding of Xdj1, whereas mitochondria deficient in either Tom20 or Tom70 were not inhibited in binding Xdj1 (Figures 1G and S2C). In mitochondria lacking Tom22, the co-purification of Xdj1 with $Tom40_{HA}$ was strongly reduced close to the background level observed with untagged Tom40 (Figure 1F). We conclude that Tom22 is required for the efficient recruitment of Xdj1 to mitochondria and to the TOM complex.

To compare the interaction of different TOM receptors with cytosolic J-proteins, we used GST-fusion proteins of Xdj1, Ydj1, and Djp1 and incubated them with digitonin-lysed mitochondria. Upon affinity purification and washing with Triton X-100 to separate the TOM receptors (Dekker et al., 1998), Xdj1 selectively co-purified Tom22 but none of the other TOM receptors (Figure 1H). Ydj1 did not co-purify any of the TOM receptors, whereas Djp1 selectively interacted with Tom70 (Figure 1H). As control, the most abundant outer membrane protein Por1 was not co-purified with any of the J-proteins. GST-Djp1 bound the purified cytosolic domain of Tom70 (Figure 1I), indicating a direct interaction between Djp1p and Tom70.

We conclude that Tom22 recruits Xdj1 to the TOM complex. In addition, Tom70 specifically binds to Djp1, revealing a direct interaction between Djp1 and Tom70 that are both involved in the biogenesis of Mim1 and further membrane proteins (Papić et al., 2013; Hansen et al., 2018; Jores et al., 2018). Thus, two cytosolic J-proteins interact with different TOM receptors.

Xdj1 Promotes Biogenesis of the TOM Complex

To analyze a potential role of Xdj1 in mitochondrial biogenesis, *xdj1*Δ cells were grown at elevated temperature on

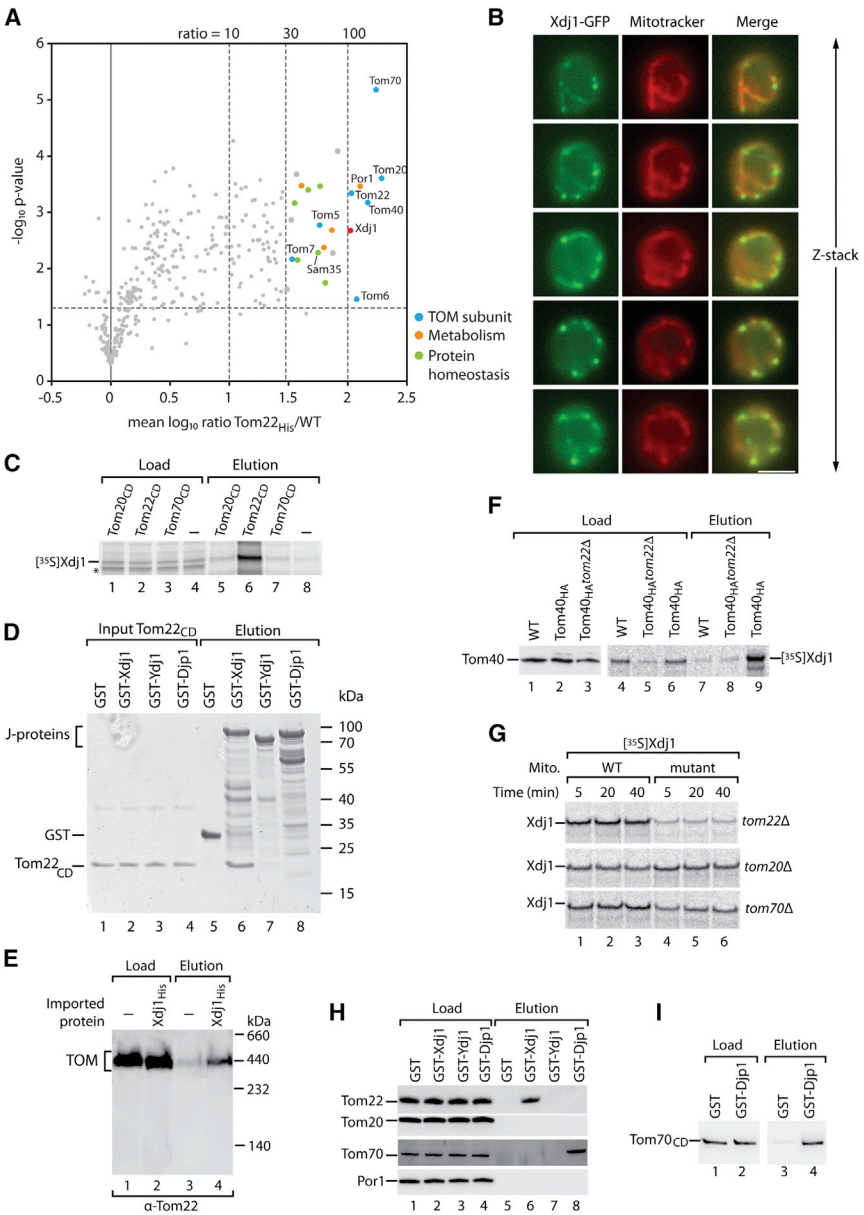

Figure 1. Xdj1 Binds to the TOM Complex via Tom22, whereas Djp1 Binds to Tom70

(A) $Tom22_{His}$ and wild-type (WT) mitochondria were subjected to affinity purification via Ni-NTA agarose. Potential interaction partners of Tom22 were identified by SILAC-based quantitative mass spectrometry. Depicted are the mean log_{10} $Tom22_{His}$ / WT ratios and the corresponding p values ($-log_{10}$-transformed; $n \geq 2$). See Table S1 for a complete list of interactors.

(B) Yeast cells expressing $Xdj1_{GFP}$ were stained with MitoTracker Deep Red and analyzed by fluorescence microscopy. Z-slices of the green fluorescence of GFP, the red fluorescence of MitoTracker, and merged images are shown. Scale bar, 5 μm.

(C) ^{35}S-labeled Xdj1 was incubated with Ni-NTA agarose and with Ni-NTA coated with the His-tagged cytosolic domains (CD) of Tom20, Tom22, or Tom70. Load (2.5%) and elution (100%) were analyzed by SDS-PAGE and autoradiography. Asterisk, non-specific band.

(D) $Tom22_{CD}$ was incubated with glutathione columns coated with GST, $_{GST}$Xdj1, $_{GST}$Ydj1, or $_{GST}$Djp1. Input (2%) and elution (50%) were analyzed by SDS-PAGE and Coomassie blue staining.

(E) $Xdj1_{His}$ was incubated with lysed mitochondria and purified via Ni-NTA agarose. Load (2%) and elution (100%) were analyzed by blue native electrophoresis and immunodetection.

(F) [^{35}S]Xdj1 was incubated with the indicated mitochondria, followed by anti-HA chromatography. Load (2%) and elution (100%) were analyzed by SDS-PAGE, immunodetection, and autography.

(G) [^{35}S]Xdj1 was incubated with *tom22*Δ, *tom20*Δ, or *tom70*Δ mitochondria and their corresponding WT mitochondria.

(H) Lysed mitochondria were incubated with glutathione Sepharose coated with GST, $_{GST}$Xdj1, $_{GST}$Ydj1, or $_{GST}$Djp1. Load (1%) and elution (100%) were analyzed by SDS-PAGE and immunodetection.

(I) $Tom70_{CD}$ was incubated with glutathione Sepharose coupled with GST or $_{GST}$Djp1. Load (5%) and elution (50%) were analyzed by SDS-PAGE and Coomassie blue staining.

See also Figures S1 and S2 and Table S1.

non-fermentable medium and mitochondria were isolated. The levels of Tom22 were significantly decreased in these *xdj1*Δ mitochondria, whereas the steady-state levels of other Tom proteins and further mitochondrial proteins were only mildly or not affected (Figure 2A). Blue native electrophoresis revealed decreased levels of the TOM complex (Figure 2B). Upon expression of plasmid-encoded Xdj1 in *xdj1*Δ cells, the levels of Tom22 and of the TOM complex were restored (Figures 2B and S3A). The levels of other outer membrane complexes such as the MIM complex and the sorting and assembly machinery (SAM) complex were not affected in *xdj1*Δ mitochondria (Figure 2C). Similarly, respiratory chain supercomplexes remained unaffected (Figure 2C).

We synthesized the ^{35}S-labeled precursor of Tom40 in a cell-free translation system (containing J-proteins and other chaperones) and studied its import into mitochondria by blue native electrophoresis. After translocation across the outer membrane through the TOM channel, the Tom40 precursor binds to the SAM complex before it assembles via intermediate II into the mature TOM complex (Wiedemann and Pfanner, 2017). The assembly of Tom40 was already retarded at the SAM stage in *xdj1*Δ mitochondria (Figure 2D). Since the levels of the SAM complex were not affected, this finding indicates that the reduced levels of the TOM complex in *xdj1*Δ mitochondria delayed the initial import step of the precursor across the outer membrane. The import of presequence-containing preproteins was similarly delayed in the *xdj1*Δ mitochondria (Figure S3B).

The assembly of Tom40 and the levels of the TOM complex were neither decreased in *ydj1*Δ nor in *djp1*Δ mitochondria (Figures 2D and 2E). In agreement with Papić et al. (2013), the levels of the assembled MIM complex were selectively reduced in

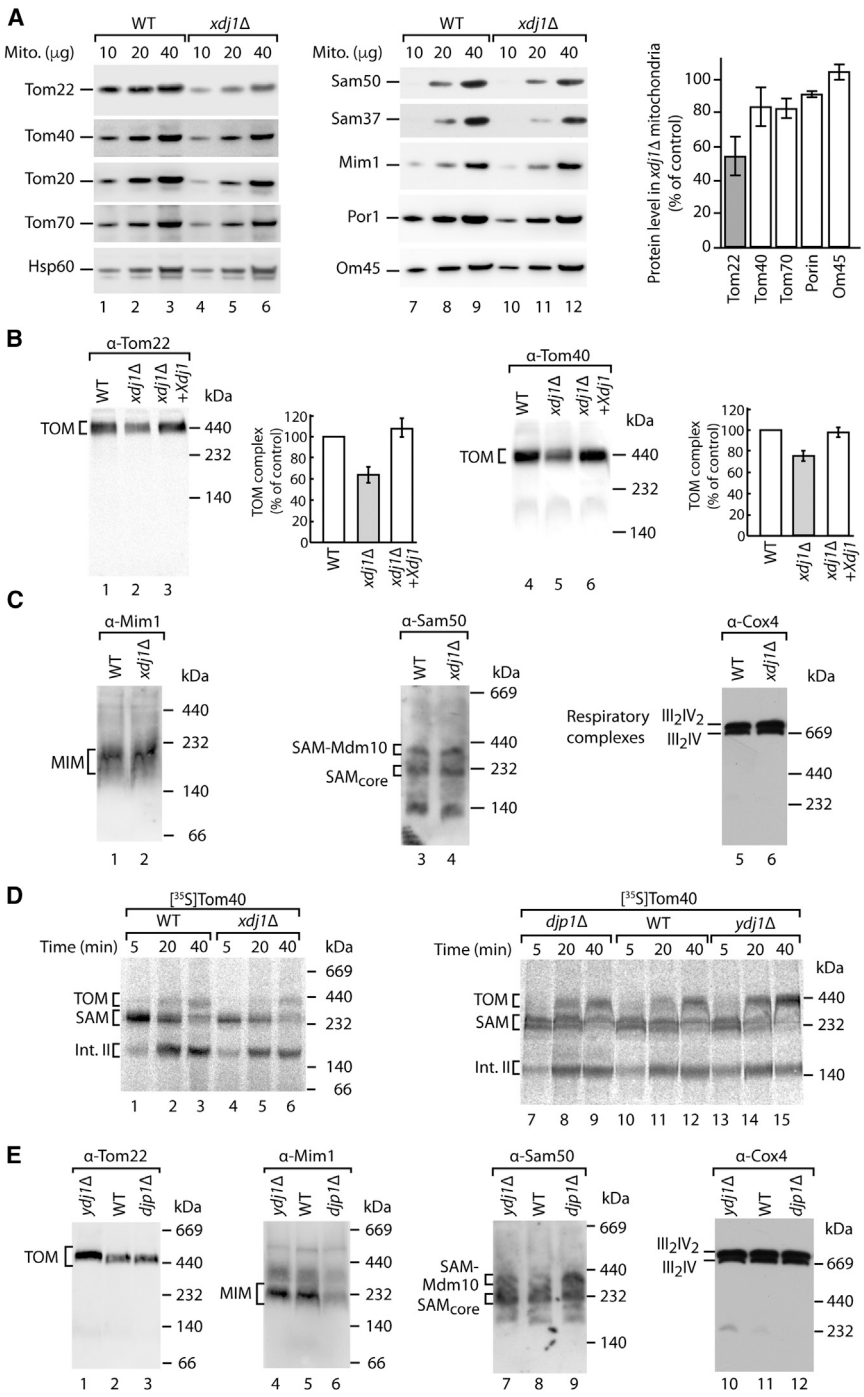

Figure 2. Xdj1 Promotes Biogenesis of the TOM Complex

(A) Wild-type (WT) and *xdj1*Δ mitochondria (protein amount) were analyzed by SDS-PAGE and immunodetection. Cells were grown at 37°C on YPG medium (1% [w/v] yeast extract, 2% [w/v] bactopeptone, 3% [w/v] glycerol). Quantification of steady-state levels of proteins in *xdj1*Δ mitochondria is shown; mean values ± SEM (n = 3–5); the levels in WT mitochondria were set to 100% (control).

(B) Mitochondria from WT, *xdj1*Δ, and an *xdj1*Δ strain expressing plasmid-encoded *XDJ1* were analyzed by blue native electrophoresis and immunodetection. Quantification and mean values of Tom22 and Tom40 in the TOM complex ± SEM (n = 3) are shown; the amount of Tom22 or Tom40 in the WT TOM complex was set to 100% (control). Mitochondria likely contain distinct populations of the TOM complex with different copy numbers of Tom subunits (Neupert and Herrmann, 2007; Wiedemann and Pfanner, 2017), visualized by a broader Tom40 blue native band in WT mitochondria (lane 4). The limiting amount of Tom22 in *xdj1*Δ mitochondria leads to an accumulation of Tom40 preferentially in the lower part of the TOM blue native band (lane 5). Upon re-expression of Xdj1, the WT mobility of Tom40 as broader ("double") blue native band is restored.

(C) WT or *xdj1*Δ mitochondria were analyzed by blue native electrophoresis and immunodetection.

(D) [^{35}S]Tom40 was imported into WT, *xdj1*Δ, *djp1*Δ, and *ydj1*Δ mitochondria and analyzed by blue native electrophoresis and autoradiography.

(E) WT, *ydj1*Δ, and *djp1*Δ mitochondria were analyzed by blue native electrophoresis and immunodetection.

See also Figure S3.

*djp1*Δ mitochondria, whereas the levels of the SAM complex and respiratory chain supercomplexes were neither decreased in *ydj1*Δ nor *djp1*Δ mitochondria (Figure 2E).

Taken together, Xdj1 and Djp1 affect the biogenesis of protein translocases of the mitochondrial outer membrane. Djp1 is involved in the biogenesis of the MIM complex (Papić et al., 2013), and Xdj1 is required for efficient assembly of the TOM complex.

Xdj1 Delivers Preproteins to the Tom22 Receptor

We asked whether Xdj1 binds to precursors of mitochondrial proteins. We incubated ^{35}S-labeled precursor proteins with GST-fusions of Xdj1, Ydj1, and Djp1 and observed an interaction of Xdj1 with precursor proteins containing hydrophobic segments such as Tom22, Oxa1, and the model preprotein b_2-DHFR, whereas only weak binding occurred to Ydj1 and Djp1 (Figure 3A). We did not detect efficient binding of hydrophilic precursor proteins such as Tim10 and the model preprotein Su9-DHFR to any of these J-proteins (Figure 3A). We used two versions of the b_2-DHFR preprotein to test the relevance of the hydrophobic segment for binding to Xdj1. b_2Δ-DHFR, which lacks the single hydrophobic segment (Brix et al., 1997), interacted with Xdj1 only very weakly, in contrast to b_2-DHFR that contains the hydrophobic segment (Figure 3B). Preincubation of *in vitro* synthesized b_2-DHFR with $_{GST}$Xdj1 stimulated import of the preprotein into wild-type

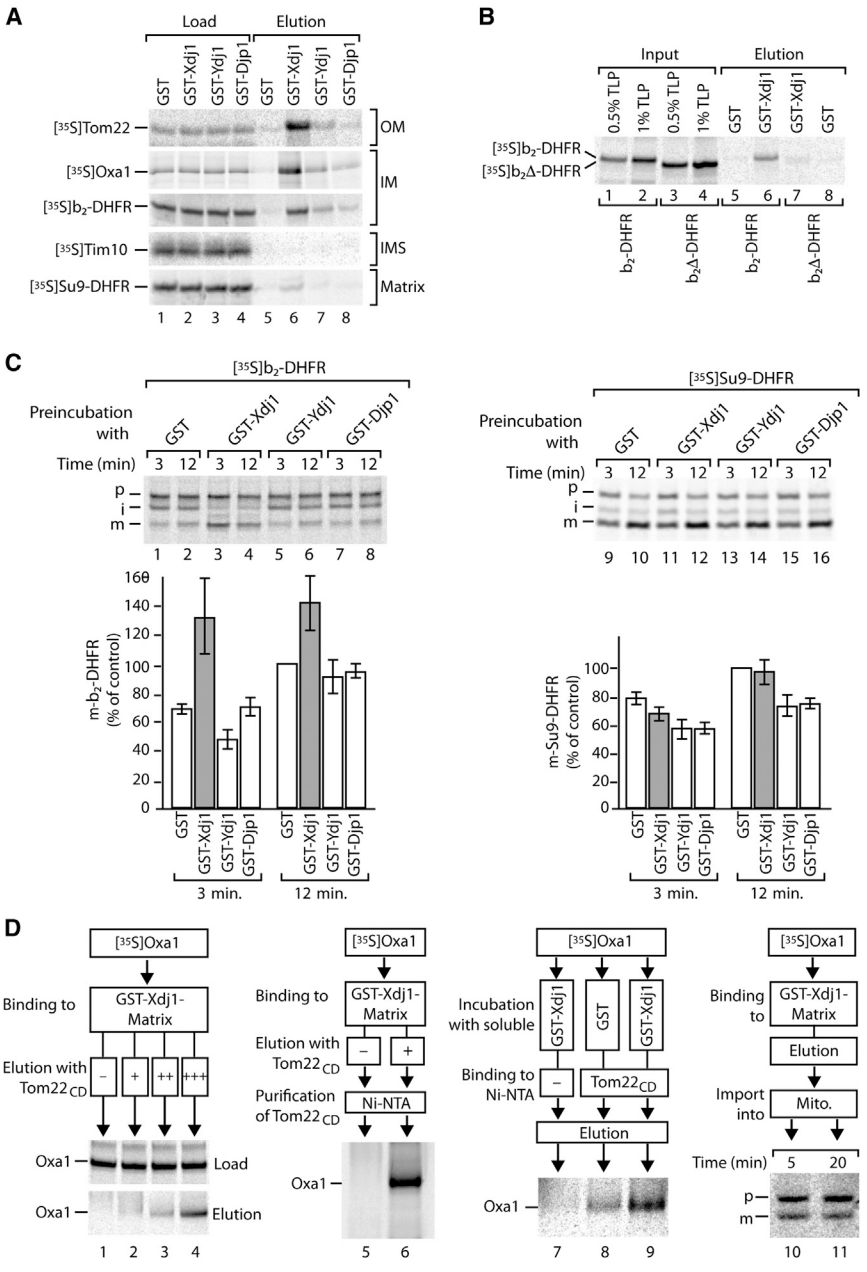

Figure 3. Xdj1 Delivers Precursor Proteins to the Tom22 Receptor

(A and B) ^{35}S-labeled precursors were incubated with glutathione Sepharose coupled with GST, $_{GST}$Xdj1, $_{GST}$Ydj1, or $_{GST}$Djp1. Load and elution fractions were analyzed by SDS-PAGE and autoradiography.

(A) Load 0.7%; elution was 33%.

(B) Input, translation product (TLP); elution was 50%.

(C) [^{35}S]b_2-DHFR and [^{35}S]Su9-DHFR precursors were incubated with GST-tagged J-proteins, followed by import into isolated wild-type mitochondria. The import reaction was analyzed by SDS-PAGE and autoradiography. p, precursor; i, intermediate; m, mature. Quantification of mature-sized proteins is shown, mean values ± SEM (n = 3–4); the import after 12 min in the presence of GST was set to 100% (control).

(D) Left panel, [^{35}S]Oxa1 precursor was incubated with glutathione Sepharose coupled with $_{GST}$Xdj1. Bound proteins were eluted with increasing amounts of His-tagged cytosolic domain (CD) of Tom22. Load was 1%; elution was 25%. Second panel, [^{35}S]Oxa1 was incubated with glutathione Sepharose coupled with $_{GST}$Xdj1. Bound proteins were incubated in the presence or absence of His-tagged $Tom22_{CD}$. The eluted proteins were purified via Ni-NTA and analyzed by SDS-PAGE and autoradiography. Third panel, [^{35}S]Oxa1 was incubated in the presence or absence of $_{GST}$Xdj1, and the binding to His-tagged $Tom22_{CD}$ was analyzed by SDS-PAGE and autoradiography. Input was 1%; elution was 100%. Right panel, [^{35}S]Oxa1 was incubated with glutathione Sepharose coupled with $_{GST}$Xdj1. Bound proteins were eluted, imported into isolated mitochondria, and analyzed by SDS-PAGE and autoradiography. p, precursor; m, mature.

mitochondria, whereas $_{GST}$Ydj1 and $_{GST}$Djp1 did not (Figure 3C). The import of Su9-DHFR was not promoted by any of the J-proteins (Figure 3C). Taken together, our findings indicate that Xdj1 binds not only to mature Tom22, but also to precursors with hydrophobic segments and promotes their import into mitochondria.

To characterize a putative transfer of preproteins from Xdj1 to Tom22, we used several experimental approaches. We set up an *in vitro* transfer assay using the Oxa1 precursor as model substrate. First, radiolabeled Oxa1 precursor was incubated with GST-fused Xdj1 coupled to glutathione Sepharose. Incubation of the Xdj1 affinity matrix with increasing amounts of the cytosolic domain of Tom22 led to an elution of the Oxa1 precursor (Figure 3D, lanes 2–4). Subsequent affinity purification of the Tom22 domain via a His tag led to co-purification of the Oxa1 precursor released from Xdj1 (Figure 3D, lane 6). Thus, the Oxa1 precursor was transferred from Xdj1 to Tom22. Second, we incubated the Oxa1 precursor in the absence or presence of soluble Xdj1 with the immobilized cytosolic domain of Tom22. Preincubation with Xdj1 considerably enhanced binding of the precursor to Tom22 (Figure 3D, lanes 8 and 9). Third, the Oxa1 precursor was bound to the GST-Xdj1 affinity column, followed by elution with reduced glutathione and incubation with isolated mitochondria, leading to import and processing to the mature Oxa1 (Figure 3D, lanes 10 and 11). We conclude that Xdj1 delivers preproteins in an import-competent form to the receptor Tom22.

Substrate-Binding Domain of Xdj1 Binds to Tom22 and J-Domain Promotes Protein Biogenesis

The 51-kDa protein Xdj1 is a type I J-protein consisting of an N-terminal J-domain, a glycine/phenylalanine rich region, two

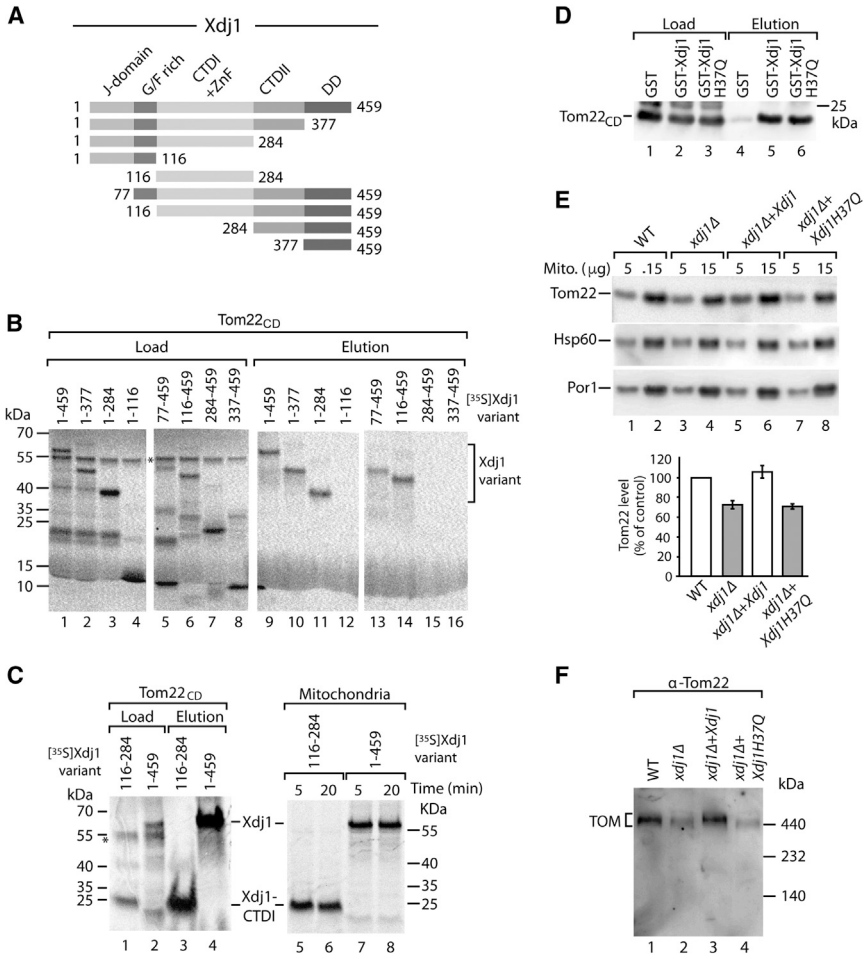

Figure 4. The Barrel Domain CTD1 of Xdj1 Binds to Tom22 and the J-Domain Promotes Protein Biogenesis

(A) Schematic view of truncated Xdj1 constructs. J-domain; G/F rich, glycine/phenylalanine rich domain; CTDI + II, C-terminal (barrel) domains I, II; ZnF, zinc finger-like region; DD, dimerization domain.

(B) Xdj1 constructs were incubated with $Tom22_{CD}$ coupled to Ni-NTA. Load and elution fractions were analyzed by SDS-PAGE and autoradiography. Load was 5%; elution was 50%.

(C) Left panel, ^{35}S-labeled Xdj1-CTDI and full-length Xdj1 were incubated with $Tom22_{CD}$ coupled to Ni-NTA. Load (5%) and elution (100%) were analyzed by SDS-PAGE and autoradiography. Right panel, Xdj1-CTDI and Xdj1 were incubated with isolated mitochondria. Mitochondria-bound proteins were analyzed by SDS-PAGE and autoradiography.

(D) $Tom22_{CD}$ was incubated with glutathione columns coated with GST, $_{GST}$Xdj1, or $_{GST}$Xdj1-H37Q. Load (2%) and elution (100%) were analyzed by SDS-PAGE and immunodetection with Tom22-specific antiserum.

(E) Mitochondria from wild-type (WT), *xdj1*Δ, and *xdj1*Δ strains expressing plasmid-encoded *XDJ1* or *XDJ1-H37Q* were analyzed by SDS-PAGE and immunodetection. Quantification of Tom22 levels, mean values ± SEM (n = 3); the amount in WT mitochondria was set to 100% (control).

(F) Mitochondria from WT, *xdj1*Δ, and *xdj1*Δ strains expressing *XDJ1* or *XDJ1-H37Q* were analyzed by blue native electrophoresis and immunodetection. See also Figure S4.

barrel domains called CTD1 and CTD2, and a C-terminal putative dimerization domain (Figure 4A) (Walsh et al., 2004; Kampinga and Craig, 2010; Sahi et al., 2013). CTD1 contains a zinc finger-like region and is required for binding client peptides (Sahi et al., 2013). We synthesized truncated versions of Xdj1 that lacked N-terminal or C-terminal domains and determined their interaction with the cytosolic domain of Tom22 (Figure 4B). Xdj1 variants lacking the J-domain, the glycine/phenylalanine rich region, CTD2 and/or the dimerization domain bound to Tom22. However, as soon as CTD1 was lacking, the binding to Tom22 was abolished (Figure 4B). We compared these *in vitro* binding assays with the interaction of [^{35}S]Xdj1 variants with mitochondria; the in organello binding assay reflected well the Tom22 binding assay (Figure S4A). *In vitro* synthesized [^{35}S] CTD1 was sufficient for binding to the cytosolic domain of Tom22 as well as to mitochondria (Figure 4C). Full-length Xdj1 variants with single amino acid exchanges in the predicted substrate-binding cleft of CTD1 (F151A, I243A) (Sahi et al., 2013) were impaired in binding to mitochondria (Figure S4B). We conclude that the barrel domain CTD1 is required for binding of Xdj1 to the receptor domain of Tom22 and the interaction with mitochondria.

J-domains interact with Hsp70 chaperones and stimulate their ATPase activity (Bukau et al., 2006; Kampinga and Craig, 2010), yet removal of the J-domain of Xdj1 did not block binding of the truncated protein to Tom22 and mitochondria (Figures 4B and S4A). Similarly, inactivation of the J-domain by an amino acid replacement in the characteristic HPD motif (Xdj1-H37Q) not or only mildly impaired binding of full-length Xdj1 to Tom22 and mitochondria (Figures 4D and S4B). However, $_{GST}$Xdj1-H37Q did not stimulate the import of b_2-DHFR into isolated mitochondria (Figure S4C) in contrast to $_{GST}$Xdj1 (Figure 3C). Expression of the Xdj1-H37Q variant did not restore the levels of Tom22 and TOM complex in mitochondria of the *xdj1*Δ strain (Figures 4E and 4F). Taken together, our results indicate that Xdj1 directly binds to Tom22 via its substrate-binding cleft and that the J-domain is required for the promotion of mitochondrial protein biogenesis by Xdj1.

DISCUSSION

We have identified the cytosolic co-chaperone Xdj1 as an interaction partner of Tom22, the central receptor of the TOM complex. The receptor domain of Tom22 selectively recruits Xdj1

from the cytosol to mitochondria. Xdj1 fulfills two functions for mitochondrial protein biogenesis. First, Xdj1 is important to maintain the levels of Tom22. Xdj1 binds to both the precursor and mature form of Tom22 and promotes the efficient formation of the TOM complex. Second, Xdj1 binds to several precursor proteins with hydrophobic segments and facilitates their transfer to the Tom22 receptor. The function of Xdj1 in mitochondrial biogenesis is supported by *in vivo* data. Cells lacking *XDJ1* show a slower growth under conditions where a high mitochondrial activity is required. The double-deletion strain *xdj1*Δ *pam17*Δ shows a synthetic growth defect and accumulation of precursor proteins (Sahi et al., 2013). A recent high-throughput study reported additional genetic interactions of *xdj1*Δ with mutants of several components of the presequence pathway (Tim17, Tim23, Tim50, Mgr2, Pam16, and Tom20) (Costanzo et al., 2016; Usaj et al., 2017).

J-proteins function as co-chaperones of the major chaperone class of Hsp70s; however, their function is not limited to stimulating the ATPase activity of Hsp70s, but various J-proteins can bind substrates themselves and are involved in a large diversity of cellular functions (Walsh et al., 2004; Kampinga and Craig, 2010). Our findings indicate that both the substrate-binding barrel domain CTD1 and the J-domain of Xd1j are involved in promoting mitochondrial protein biogenesis. The CTD1 domain of Xdj1 directly interacts with the receptor domain of Tom22. A functional J-domain is required for the promotion of mitochondrial protein biogenesis in agreement with the view that Xdj1 cooperates with cytosolic Hsp70 in protein delivery to mitochondria. J-proteins transiently interact with Hsp70 proteins, explaining why Xdj1, but not Hsp70, was found as a top hit in the mass-spectrometry-based screen for Tom22 interactors (Figure 1A; Table S1). Xdj1 is a low abundant J-protein with about 500–600 copies per yeast cell, an order of magnitude below the copy number of the TOM complex (Sahi et al., 2013; Morgenstern et al., 2017) and is distributed between cytosol and mitochondria. Taken together, the findings suggest that Xdj1 dynamically interacts with the TOM complex and exerts a catalytic role in mitochondrial protein biogenesis.

Xdj1 is not the only cytosolic J-protein that is specifically recruited to the mitochondrial surface. We observed that Djp1 selectively interacts with the receptor Tom70. It has been shown that Djp1 binds to several newly synthesized mitochondrial membrane proteins in the cytosol and at the surface of the endoplasmic reticulum and that both Djp1 and Tom70 are required for efficient import of the precursors into mitochondria (Papić et al., 2013; Hansen et al., 2018; Jores et al., 2018), yet the molecular mechanism of cooperation of Djp1 and Tom70 has been open. We conclude that the direct binding of Djp1 to Tom70 promotes the transfer of hydrophobic precursor proteins into mitochondria.

We propose that a receptor-mediating docking mechanism of cytosolic J-proteins contributes to the specificity and efficiency of membrane targeting processes. Xdj1 and Djp1 interact with distinct TOM receptors to promote the biogenesis of mitochondrial outer membrane translocases and the import of precursor proteins. These co-chaperones directly bind to the receptors, emphasizing a specific role of the J-proteins in addition to the stimulation of Hsp70s.

STAR★METHODS

Detailed methods are provided in the online version of this paper and include the following:

- KEY RESOURCES TABLE
- CONTACT FOR REAGENT AND RESOURCE SHARING
- EXPERIMENTAL MODEL AND SUBJECT DETAILS
- METHOD DETAILS
  - Yeast strains and growth
  - Purification of GST-fusion constructs
  - Isolation of mitochondria
  - Submitochondrial localization
  - *In vitro* protein import into mitochondria
  - Affinity purification for mass spectrometry
  - Mass spectrometry
  - Binding assay to isolated mitochondria
  - Import stimulation assay
  - *In vitro* binding to TOM receptors
  - Affinity purification of $Tom40_{HA}$
  - Purification via Glutathione Sepharose
  - Precursor transfer assay
  - Microscopy
  - Miscellaneous
- QUANTIFICATION AND STATISTICAL ANALYSIS
- DATA AND SOFTWARE AVAILABIITY

SUPPLEMENTAL INFORMATION

Supplemental Information includes four figures and two tables and can be found with this article online at https://doi.org/10.1016/j.celrep.2018.10.083.

ACKNOWLEDGMENTS

We thank Nicole Zufall for expert technical assistance. Work included in this study has also been performed in partial fulfillment of the requirements for the doctoral thesis of C.P. at the University of Freiburg. This work was supported by the Deutsche Forschungsgemeinschaft (BE 4679/2-1; PF 202/8-1 and 202/9-1), Sonderforschungsbereich 746, Research Training Group RTG 2202, Excellence Initiative of the German Federal & State Governments (EXC 294 BIOSS; GSC-4 Spemann Graduate School), the European Research Council (ERC) Consolidator Grant no. 648235, and an EMBO long-term fellowship (to L.O.).

AUTHOR CONTRIBUTIONS

L.O., J.S., C.P., L.-S.W., and S.O. performed the experiments and analyzed data together with B.W., T.B., and N.P.; T.B., N.P., and L.O. designed and supervised the project; L.O., J.S., S.O., and T.B. prepared the figures; N.P. and T.B. wrote the manuscript; and all authors discussed results from the experiments and commented on the manuscript.

DECLARATION OF INTERESTS

The authors declare no competing interests.

Received: November 26, 2017
Revised: September 19, 2018
Accepted: October 24, 2018
Published: November 20, 2018

REFERENCES

Atencio, D.P., and Yaffe, M.P. (1992). MAS5, a yeast homolog of DnaJ involved in mitochondrial protein import. Mol. Cell. Biol. *12*, 283–291.

Becker, J., Walter, W., Yan, W., and Craig, E.A. (1996). Functional interaction of cytosolic hsp70 and a DnaJ-related protein, Ydj1p, in protein translocation *in vivo*. Mol. Cell. Biol. *16*, 4378–4386.

Becker, T., Wenz, L.S., Krüger, V., Lehmann, W., Müller, J.M., Goroncy, L., Zufall, N., Lithgow, T., Guiard, B., Chacinska, A., et al. (2011). The mitochondrial import protein Mim1 promotes biogenesis of multispanning outer membrane proteins. J. Cell Biol. *194*, 387–395.

Böttinger, L., Oeljeklaus, S., Guiard, B., Rospert, S., Warscheid, B., and Becker, T. (2015). Mitochondrial heat shock protein (Hsp) 70 and Hsp10 cooperate in the formation of Hsp60 complexes. J. Biol. Chem. *290*, 11611–11622.

Brix, J., Dietmeier, K., and Pfanner, N. (1997). Differential recognition of preproteins by the purified cytosolic domains of the mitochondrial import receptors Tom20, Tom22, and Tom70. J. Biol. Chem. *272*, 20730–20735.

Bukau, B., Weissman, J., and Horwich, A. (2006). Molecular chaperones and protein quality control. Cell *125*, 443–451.

Caplan, A.J., Cyr, D.M., and Douglas, M.G. (1992). YDJ1p facilitates polypeptide translocation across different intracellular membranes by a conserved mechanism. Cell *71*, 1143–1155.

Christianson, T.W., Sikorski, R.S., Dante, M., Shero, J.H., and Hieter, P. (1992). Multifunctional yeast high-copy-number shuttle vectors. Gene *110*, 119–122.

Costanzo, M., VanderSluis, B., Koch, E.N., Baryshnikova, A., Pons, C., Tan, G., Wang, W., Usaj, M., Hanchard, J., Lee, S.D., et al. (2016). A global genetic interaction network maps a wiring diagram of cellular function. Science *353*, aaf1420.

Cox, J., and Mann, M. (2008). MaxQuant enables high peptide identification rates, individualized p.p.b.-range mass accuracies and proteome-wide protein quantification. Nat. Biotechnol. *26*, 1367–1372.

Cox, J., Neuhauser, N., Michalski, A., Scheltema, R.A., Olsen, J.V., and Mann, M. (2011). Andromeda: A peptide search engine integrated into the MaxQuant environment. J. Proteome Res. *10*, 1794–1805.

Dekker, P.J.T., Ryan, M.T., Brix, J., Müller, H., Hönlinger, A., and Pfanner, N. (1998). Preprotein translocase of the outer mitochondrial membrane: Molecular dissection and assembly of the general import pore complex. Mol. Cell. Biol. *18*, 6515–6524.

Ellenrieder, L., Opaliński, Ł., Becker, L., Krüger, V., Mirus, O., Straub, S.P., Ebell, K., Flinner, N., Stiller, S.B., Guiard, B., et al. (2016). Separating mitochondrial protein assembly and endoplasmic reticulum tethering by selective coupling of Mdm10. Nat. Commun. *7*, 13021.

Endo, T., and Yamano, K. (2010). Transport of proteins across or into the mitochondrial outer membrane. Biochim. Biophys. Acta *1803*, 706–714.

Hansen, K.G., Aviram, N., Laborenz, J., Bibi, C., Meyer, M., Spang, A., Schuldiner, M., and Herrmann, J.M. (2018). An ER surface retrieval pathway safeguards the import of mitochondrial membrane proteins in yeast. Science *361*, 1118–1122.

Hoseini, H., Pandey, S., Jores, T., Schmitt, A., Franz-Wachtel, M., Macek, B., Buchner, J., Dimmer, K.S., and Rapaport, D. (2016). The cytosolic cochaperone Sti1 is relevant for mitochondrial biogenesis and morphology. FEBS J. *283*, 3338–3352.

Itakura, E., Zavodszky, E., Shao, S., Wohlever, M.L., Keenan, R.J., and Hegde, R.S. (2016). Ubiquilins chaperone and triage mitochondrial membrane proteins for degradation. Mol. Cell *63*, 21–33.

Jores, T., Lawatscheck, J., Beke, V., Franz-Wachtel, M., Yunoki, K., Fitzgerald, J.C., Macek, B., Endo, T., Kalbacher, H., Buchner, J., and Rapaport, D. (2018). Cytosolic Hsp70 and Hsp40 chaperones enable the biogenesis of mitochondrial β-barrel proteins. J. Cell Biol. *217*, 3091–3108.

Kampinga, H.H., and Craig, E.A. (2010). The HSP70 chaperone machinery: J proteins as drivers of functional specificity. Nat. Rev. Mol. Cell Biol. *11*, 579–592.

Knop, M., Siegers, K., Pereira, G., Zachariae, W., Winsor, B., Nasmyth, K., and Schiebel, E. (1999). Epitope tagging of yeast genes using a PCR-based strategy: More tags and improved practical routines. Yeast *15* (*10B*), 963–972.

Morgenstern, M., Stiller, S.B., Lübbert, P., Peikert, C.D., Dannenmaier, S., Drepper, F., Weill, U., Höß, P., Feuerstein, R., Gebert, M., et al. (2017). Definition of a high-confidence mitochondrial proteome at quantitative scale. Cell Rep. *19*, 2836–2852.

Müller, C.S., Bildl, W., Haupt, A., Ellenrieder, L., Becker, T., Hunte, C., Fakler, B., and Schulte, U. (2016). Cryo-slicing Blue Native-Mass Spectrometry (csBN-MS), a Novel Technology for High Resolution Complexome Profiling. Mol. Cell. Proteomics *15*, 669–681.

Neupert, W., and Herrmann, J.M. (2007). Translocation of proteins into mitochondria. Annu. Rev. Biochem. *76*, 723–749.

Ong, S.E., Blagoev, B., Kratchmarova, I., Kristensen, D.B., Steen, H., Pandey, A., and Mann, M. (2002). Stable isotope labeling by amino acids in cell culture, SILAC, as a simple and accurate approach to expression proteomics. Mol. Cell. Proteomics *1*, 376–386.

Papić, D., Elbaz-Alon, Y., Koerdt, S.N., Leopold, K., Worm, D., Jung, M., Schuldiner, M., and Rapaport, D. (2013). The role of Djp1 in import of the mitochondrial protein Mim1 demonstrates specificity between a cochaperone and its substrate protein. Mol. Cell. Biol. *33*, 4083–4094.

Sahi, C., Kominek, J., Ziegelhoffer, T., Yu, H.Y., Baranowski, M., Marszalek, J., and Craig, E.A. (2013). Sequential duplications of an ancient member of the DnaJ-family expanded the functional chaperone network in the eukaryotic cytosol. Mol. Biol. Evol. *30*, 985–998.

Schleiff, E., and Becker, T. (2011). Common ground for protein translocation: Access control for mitochondria and chloroplasts. Nat. Rev. Mol. Cell Biol. *12*, 48–59.

Schwarz, E., Westermann, B., Caplan, A.J., Ludwig, G., and Neupert, W. (1994). XDJ1, a gene encoding a novel non-essential DnaJ homologue from *Saccharomyces cerevisiae*. Gene *145*, 121–124.

Sikorski, R.S., and Hieter, P. (1989). A system of shuttle vectors and yeast host strains designed for efficient manipulation of DNA in *Saccharomyces cerevisiae*. Genetics *122*, 19–27.

Usaj, M., Tan, Y., Wang, W., VanderSluis, B., Zou, A., Myers, C.L., Costanzo, M., Andrews, B., and Boone, C. (2017). TheCellMap.org: A web-accessible database for visualizing and mining the global yeast genetic interaction network. G3: Gene. G3 (Bethesda) *7*, 1539–1549.

Vizcaíno, J.A., Csordas, A., del-Toro, N., Dianes, J.A., Griss, J., Lavidas, I., Mayer, G., Perez-Riverol, Y., Reisinger, F., Ternent, T., et al. (2016). 2016 update of the PRIDE database and its related tools. Nucleic Acids Res. *44* (*D1*), D447–D456.

Walsh, P., Bursać, D., Law, Y.C., Cyr, D., and Lithgow, T. (2004). The J-protein family: Modulating protein assembly, disassembly and translocation. EMBO Rep. *5*, 567–571.

Wiedemann, N., and Pfanner, N. (2017). Mitochondrial machineries for protein import and assembly. Annu. Rev. Biochem. *86*, 685–714.

Williams, C.C., Jan, C.H., and Weissman, J.S. (2014). Targeting and plasticity of mitochondrial proteins revealed by proximity-specific ribosome profiling. Science *346*, 748–751.

Young, J.C., Hoogenraad, N.J., and Hartl, F.U. (2003). Molecular chaperones Hsp90 and Hsp70 deliver preproteins to the mitochondrial import receptor Tom70. Cell *112*, 41–50.

Zahedi, R.P., Sickmann, A., Boehm, A.M., Winkler, C., Zufall, N., Schönfisch, B., Guiard, B., Pfanner, N., and Meisinger, C. (2006). Proteomic analysis of the yeast mitochondrial outer membrane reveals accumulation of a subclass of preproteins. Mol. Biol. Cell *17*, 1436–1450.

STAR★METHODS

KEY RESOURCES TABLE

REAGENT or RESOURCE	SOURCE	IDENTIFIER
Antibodies		
Rabbit polyclonal anti-Cox4	Böttinger et al., 2015	GR578-4
Rabbit polyclonal anti-mtHsp70	Böttinger et al., 2015	GR2055-KB
Rabbit polyclonal anti-Tim23	Böttinger et al., 2015	133-4
Rabbit polyclonal anti-Tim44	Böttinger et al., 2015	128-4
Rabbit polyclonal anti-Om14	Ellenrieder et al., 2016	GR3040-6
Rabbit polyclonal anti-Sam37	Ellenrieder et al., 2016	161-8
Rabbit polyclonal anti-Sam50	Ellenrieder et al., 2016	312-17
Rabbit polyclonal anti-Mim1	Ellenrieder et al., 2016	GR1837-5
Rabbit polyclonal anti-Om45	Ellenrieder et al., 2016	GR1311-4
Rabbit polyclonal anti-Por1	This paper	GR3621-5
Rabbit polyclonal anti-Hsp60	Böttinger et al., 2015	170 (60)
Rabbit polyclonal anti-Tom20	Ellenrieder et al., 2016	GR3225-7
Rabbit polyclonal anti-Tom22	Ellenrieder et al., 2016	GR3227-2
Rabbit polyclonal anti-Tom40	Ellenrieder et al., 2016	168-5
Rabbit polyclonal anti-Tom70	Ellenrieder et al., 2016	GR657-3
Anti-HA peptide, mouse monoclonal antibody, clone 12Ca5	Roche	RRID: AB_514505; Cat. 11583816001
Anti-Penta-His, mouse antibody	QIAGEN	RRID: AB_2619735; Cat. 34660
Goat Peroxidase-coupled anti-Rabbit IgG	Jackson ImmunoResearch Laboratories	RRID: AB2313567; Cat. #111-035-003
Goat Peroxidase-coupled anti-Mouse IgG	Sigma	RRID: AB_258167; Cat. A4416
Chemicals, Peptides, and Recombinant Proteins		
L-[^{35}S]-Methionine	PerkinElmer	Cat. #NEG009005MC
MitoTracker Deep Red	Invitrogen	Cat. M22426
Glutathione S-Sepharose 4B	GE Healthcare	Cat. 17075601
Anti-HA affinity matrix	Roche	Cat. #11815016001
Ni-NTA Agarose	QIAGEN	Cat. #30230
Critical Commercial Assays		
TNT® Quick Coupled Reaction Mix	Promega	Cat. #L2080
Roti®-Quant Bradford reagent	Roth	Cat. #K015.3
KOD Hot Start Master Mix	Merck Millipore	Cat. #71842-3
RedTaq Polymerase PCR Master Mix (2x)	Genaxxon Bioscience	Cat. #M3029.0500
mMessage mMachine SP6 Transcription Kit	Thermo Fisher Scientific	Cat. #AM1340
MEGAclear Transcription Clean-Up Kit	Thermo Fisher Scientific	Cat. #AM1908
Experimental Models: Organisms/Strains		
YPH499 (WT) *MATa ura3-52 lys2-801_amber ade2-101_ochre trp1-Δ63 his3-Δ200 leu2-Δ1*	Sikorski and Hieter, 1989	1501
YPH499 (WT) rho-	Becker et al., 2011	1519
YPH499 rho- pRS415-*TOM40HA*	Becker et al., 2011	3177
YPH499 rho- *Tom22::HIS3* pRS415-*TOM40HA*	Becker et al., 2011	3178
YPH499 *arg4::kanMX4*	This paper	2799
YPH499 *tom22:TOM22HIS arg4::kanMX4*	This paper	3955
YPH499 *tom20::URA3* pYep13-*TOM22*	Becker et al., 2011	1273
YPH499 *tom70::HIS3MX6*	Becker et al., 2011	1059
YPH499 rho-*Tom22::HIS3*	Becker et al., 2011	2298

(*Continued on next page*)

Continued

REAGENT or RESOURCE	SOURCE	IDENTIFIER
BY4741 (WT) *MATa his3Δ1 leu2Δ0 met15Δ0 ura3Δ0*	EUROSCARF	1354
BY4741 *xdj1:: kanMX4*	EUROSCARF	3868
BY4741 *djp1::KanMX4*	EUROSCARF	3870
BY4741 *ydj1::KanMX4*	EUROSCARF	3869
BY4741 *xdj1:: XDJ1HA-HIS3MX6*	This paper	4447
BY4741 *pUG-XDJ1GFP*	This paper	4444
BY4741 pRS416	This paper	5277
BY4741 *xdj1::kanMX4 pRS416*	This paper	5278
BY4741 *xdj1::kanMX4* pRS416-*XDJ1*	This paper	5280
BY4741 *xdj1::kanMX4* pRS416-*XDJ1H37Q*	This paper	5315
Oligonucleotides		
See Table S2 for oligonucleotide sequences		N/A
Recombinant DNA		
pGEM4Z-*TOM40* (*S.cerevisiae)*	Pfanner/Becker Labs	1495
pGEM4Z-*CYB2*(167)-DHFR (*S. cerevisiae*)	Pfanner/Becker Labs	B03
pGEM4Z-*CYB2*(167)Δ47-65-DHFR (*S. cerevisiae*)	Pfanner/Becker Labs	B04
pGEM4Z-*TIM10* (*S. cerevisiae*)	Pfanner/Becker Labs	1235
pGEM4Z-Su9-DHFR (Su9 (1-69, *N. crassa*)-DHFR (mouse))	Pfanner/Becker Labs	S02
pGEM5X2	GE Healthcare	Cat. GE28-9545-54
pGEX5X2-*XDJ1* (*S. cerevisiae)*	This paper	2576
pGEX5X2-*XDJ1H37Q* (*S. cerevisiae)*	This paper	2577
pGEX5X2-*DJP1* (*S. cerevisiae)*	This paper	2580
pGEX5X2-*YDJ1* (*S. cerevisiae)*	This paper	2579
pUG35-*XDJ-GFP1* (*S. cerevisiae)*	This paper	2573
pRS416	Christianson et al., 1992	X 25
pRS416-*XDJ1 (S.cerevisiae)*	This paper	3112
pRS416-*XDJ1-H37Q* (*S. cerevisiae)*	This paper	3113
pFA6a-3xHA-HIS3MX6 (*S. cerevisiae)*	Knop et al., 1999	1450; pYM2
pET19b-$TOM20_{CD}HIS_{10}$ *(S.cerevisiae)*	Brix et al., 1997	1811
pET19b-$TOM22_{CD}HIS_{10}$ *(S.cerevisiae)*	Brix et al., 1997	1054
pET19b-$TOM70_{CD}HIS_{10}$ *(S.cerevisiae)*	Brix et al., 1997	1055
Software and Algorithms		
ImageJ	National Institue of Health, USA	https://imagej.nih.gov/ij/
Multi Gauge v.3.2	FujiFilm	N/A
Cell P	Olympus	N/A

CONTACT FOR REAGENT AND RESOURCE SHARING

Further information and requests for resources and reagents should be directed to and will be fulfilled by the Lead Contact, Nikolaus Pfanner (nikolaus.pfanner@biochemie.uni-freiburg.de).

EXPERIMENTAL MODEL AND SUBJECT DETAILS

Derivatives of the *S. cerevisiae* strains YPH499 and BY4741 were used in this study. Yeast strains and their corresponding genotypes are described in the KEY RESOURCES TABLE. Yeast cells were grown in YPG medium (1% [w/v] yeast extract; 2% [w/v] bacto-peptone, 3% [w/v] glycerol), YPS (1% [w/v] yeast extract; 2% [w/v] bacto-peptone, 3% [w/v] glycerol) or selective complete medium (SM) (0.67% [w/v] yeast nitrogen base; 0.07% [w/v] amino acid mixture) with 3% [w/v] glycerol and 0.1%–0.2% [w/v] glucose as carbon source. Cultures were incubated at 23-37°C under constant shaking. Cells were harvested at an early exponential growth phase. The growth phase was determined by the optical density of the culture at a wavelength of 600 nm (OD_{600}).

METHOD DETAILS

Yeast strains and growth

The yeast strains *xdj1*Δ (3868), *djp1*Δ (3870), *ydj1*Δ (3869) and their corresponding wild-type BY4741 (1354) were obtained from Euroscarf. The strains $Tom40_{HA}$ (3177), $Tom40_{HA}$ *tom22*Δ (3178) and the corresponding rho^- wild-type YPH499 (1519) were reported (Becker et al., 2011). For *in vivo* rescue experiments, we expressed *XDJ1* from a pRS416 plasmid under control of its own promoter and terminator in the *xdj1*Δ strain. To generate an Xdj1-GFP fusion construct, the full-length open reading frame of *XDJ1* lacking the stop codon was inserted into a pUG35 plasmid. The expression of $Xdj1_{GFP}$ was under control of a MET25 promoter. The construct was introduced into BY4741 yeast and positive clones were selected via a *URA3* marker of the plasmid. To generate the $Xdj1_{HA}$ strain (4447), the genetic information of a triple HA-tag was introduced before the stop-codon of *XDJ1* utilizing a *HIS3* selection marker. For SILAC-studies, we disrupted the *ARG4* gene by homologous recombination with a *kanMX4* marker in the YPH499 $Tom22_{His}$ background (3955). The corresponding YPH499 *arg4*Δ strain (2799) was reported (Böttinger et al., 2015). Strains were grown on YPG (1% (w/v) yeast extract, 2% (w/v) bacterial peptone and 3% (v/v) glycerol) medium at 24-37°C. Yeast cells expressing Xdj1 from a pRS416 plasmid were grown at 30°C in selective medium lacking uracil and containing 2% (w/v) glucose and then shifted to growth at 39°C in YPG medium. For growth analysis, a serial dilution of yeast cells were spotted on YPG or YPD (1% (w/v) yeast extract, 2% (w/v) bacterial peptone and 2% (w/v) glucose) agar plates and growth was monitored at 37°C.

Purification of GST-fusion constructs

To generate proteins N-terminally fused to GST, the open reading frames of *XDJ1*, *DJP1* and *YDJ1* were amplified via PCR and cloned into a pGEX5X2 vector (GE Healthcare) by using the BamHI and XmaI restriction sites. We used digestion with restriction enzymes and molecular sequencing to control the success of the cloning. The plasmids were transformed into *Escherichia coli* BL21 DE3 pLys cells. Bacterial cells were grown in LB medium at 37°C to an OD_{600} of 1.8. After cooling the culture to 19°C, the protein production was induced by addition of isopropyl β-D-1-thiogalactopyranoside (IPTG) to 1 mM final concentration. Subsequently, cultures were incubated for 16 h at 19°C under vigorous shaking. Cells were pelleted, resuspended in lysis buffer (50 mM Tris/HCl pH 8, 150 mM NaCl, 0.025% (v/v) Triton X-100 and 1 mM PMSF) and sonicated to open the cells. Insoluble material was removed by centrifugation (1 h, 17,000 x g, 4°C). The supernatant was applied to Glutathione Sepharose 4B (GE Healthcare) and incubated for 1 h at 4°C under constant rotation. The affinity matrix was washed with an excess amount of lysis buffer before the proteins were eluted with 50 mM Tris/HCl, pH 7.5, 150 mM NaCl, 15 mg/ml reduced glutathione. The purity of the isolated proteins was controlled by SDS-PAGE and Coomassie staining.

Isolation of mitochondria

Mitochondria were isolated by differential centrifugation (Ellenrieder et al., 2016). Yeast cells were grown to an early logarithmic growth phase and harvested by centrifugation. Cells were washed and the cell wall was digested by incubation with zymolase (3 mg/g cells) for 30 min at 30°C in zymolase buffer (1.2 M sorbitol; 20 mM KP_i, pH 7.4). Subsequently, the plasma membrane was disrupted by mechanical force in homogenization buffer (0.6 M sorbitol; 1 mM EDTA; 0.2% [w/v] bovine serum albumin; 1 mM phenylmethylsulfonyl fluoride (PMSF); 10 mM Tris/HCl, pH 7.4) using a Teflon glass homogenizer. Cell debris and nuclei were pelleted by centrifugation (2,000xg, 5 min, 4°C). The supernatant was subjected to a second centrifugation step (13,000xg, 15 min, 4°C) to collect mitochondria. The mitochondrial pellet was washed with SEM buffer (10 mM MOPS/KOH, pH 7.2, 1 mM EDTA and 250 mM sucrose) and resuspended in SEM buffer. Aliquots were shock frozen in liquid nitrogen and stored at −80°C until use.

Submitochondrial localization

The submitochondrial localization of Xdj1 was determined by a protease-accessibility assay. Intact $Xdj1_{HA}$ mitochondria were incubated with proteinase K (30 μg/ml final concentration) for 20 min on ice in SEM buffer. The protease was inactivated by addition of phenylmethylsulfonyl fluoride (PMSF) to a final concentration of 1 mM and further incubation for 10 min on ice. To disrupt the outer membrane, $Xdj1_{HA}$ mitochondria were resuspended in EM buffer (1 mM EDTA, 10 mM MOPS/KOH, pH 7.2) and treated with proteinase K.

In vitro protein import into mitochondria

^{35}S-labeled precursor proteins were synthesized in a cell-free translation system based on reticulocyte lysate (TNT kit, Promega) in the presence of ^{35}S-labeled methionine. The ^{35}S-labeled precursor proteins were incubated with isolated mitochondria in import buffer (3% (w/v) BSA, 250 mM sucrose, 5 mM methionine, 80 mM KCl, 5 mM $MgCl_2$, 10 mM MOPS/KOH, pH 7.2, and 2 mM KH_2PO_4) containing 4 mM ATP, 4 mM NADH, 5 mM creatine phosphate and 0.1 μg/ml creatine kinase. The import reaction was stopped by transfer on ice. For analysis on SDS-PAGE, non-imported precursor proteins were removed by a subsequent incubation with 50 μg/ml proteinase K for 10 min on ice. Subsequently, the protease was inactivated by incubation with 2 mM PMSF for 5 min on ice. Mitochondria were reisolated and lysed under denaturing conditions with Laemmli buffer and proteins were separated by SDS-PAGE. For blue native electrophoresis, mitochondria were reisolated and washed with SEM buffer. The mitochondrial pellet was resuspended in digitonin buffer (20 mM Tris/HCl, pH 7.4, 50 mM NaCl, 0.1 mM EDTA, 10% (v/v) glycerol) containing 1% (v/v)

digitonin and incubated on ice. After a clarifying spin the supernatant was subjected to blue native electrophoresis (Dekker et al., 1998).

Affinity purification for mass spectrometry

$Tom22_{His}$ *arg4*Δ cells and the corresponding YPH499 *arg4*Δ (wild-type) cells were grown in minimal medium (0.067% (w/v) bacto-yeast nitrogen base, amino acid mix) containing 3% (v/v) glycerol and 0.2% (w/v) glucose as carbon source. For differential labeling with amino acids the media were supplemented either with $^{14}N_2{}^{12}C_6$-lysine and $^{14}N_4{}^{12}C_6$-arginine ($Tom22_{His}$) or with $^{15}N_2{}^{13}C_6$-lysine and $^{14}N_4{}^{13}C_6$-arginine (wild-type). Mitochondria were isolated following the standard procedure described above. Isolated mitochondria were lysed with digitonin buffer containing 1% (w/v) digitonin and 10 mM imidazole. Insoluble material was removed by centrifugation. The supernatant was incubated with Ni-NTA agarose (QIAGEN) for 1 h at 4°C under constant rotation. The affinity matrix was washed with an excess amount of digitonin buffer containing 0.1% (w/v) digitonin and 40 mM imidazole. Bound proteins were eluted with digitonin buffer containing 0.1% (w/v) digitonin and 250 mM imidazole. The elution fractions of wild-type and $Tom22_{His}$ mitochondria were pooled and subjected to mass spectrometry. The experiment was performed in three biological replicates.

Mass spectrometry

Proteins were precipitated using acetone and resuspended in 60% (v/v) methanol, 20 mM NH_4HCO_3 followed by reduction and alkylation of cysteine residues with 100 mM DTT (30 min at 65°C) and 50 mM iodoacetamide (30 min at room temperature in the dark), respectively, and tryptic digestion (37°C, overnight). Peptides were analyzed by high-performance liquid chromatography/mass spectrometry on an LTQ-Orbitrap XL instrument (Thermo Scientific, Bremen, Germany) directly coupled to an UltiMate 3000 RSLCnano HPLC system (Thermo Scientific, Dreieich, Germany) (Böttinger et al., 2015).

Binding assay to isolated mitochondria

^{35}S-labeled Xdj1 and Xdj1 constructs were incubated with isolated mitochondria in import buffer. The reaction was stopped by transfer on ice. Mitochondria were reisolated and washed with SEM buffer. The mitochondrial pellet was lysed with digitonin buffer containing 1% (w/v) digitonin as described above. Insoluble material was removed by centrifugation. The supernatant was analyzed by SDS-PAGE. To identify interaction partners of Xdj1, recombinant amounts of His-tagged Xdj1 were produced in a cell-free translation system based on wheat germ (5Prime). $Xdj1_{His}$ was incubated with isolated mitochondria. After reisolation of mitochondria and a washing step with SEM buffer, mitochondria were lysed with digitonin buffer containing 1% (w/v) digitonin. Binding to Ni-NTA agarose was allowed for 1 h at 4°C. Subsequently, beads were washed with digitonin buffer containing 0.1% (w/v) digitonin and 20 mM imidazole. To elute bound proteins, the affinity matrix was incubated with digitonin buffer containing 1% (w/v) digitonin and 250 mM imidazole for 10 min on ice. Protein complexes were analyzed by blue native electrophoresis.

Import stimulation assay

For the *in vitro* import stimulation assay, radiolabeled precursors were produced in a translational extract and incubated with GST-tagged J-proteins in GST buffer for 30 min at 25°C before the import reaction. Subsequently, the precursor proteins were imported into isolated wild-type mitochondria as described above. While titrating the amount of GST-tagged Xdj1, we noticed that large amounts of $_{GST}$Xdj1 impair import of the precursors proteins in agreement with the observation that overexpression of Xdj1 is toxic for yeast cells (Sahi et al., 2013). Both an intact J-domain and substrate-binding domain are required for a toxicity of Xdj1 overexpression (Sahi et al., 2013) in agreement with our finding that both domains of Xdj1 are needed for its role in promoting mitochondrial protein biogenesis at physiological levels of expression.

In vitro binding to TOM receptors

The cytosolic domains (CD) of Tom22, Tom20 and Tom70 were recombinantly expressed and purified (Brix et al., 1997; Becker et al., 2011). Similar amounts of $Tom22_{CD}$, $Tom20_{CD}$ and $Tom70_{CD}$ were rebound to Ni-NTA agarose and incubated with ^{35}S-labeled full-length Xdj1 or various Xdj1 variants in binding buffer (20 mM Tris/HCl, pH 7.4, 0.1% (w/v) digitonin, 10 mM imidazole, 100 mM NaCl, 1 mM EDTA, 10% (v/v) glycerol) for 1 h at 4°C. The affinity matrix was washed with an excess amount of binding buffer containing 20 mM imidazole. Bound proteins were eluted with binding buffer containing 500 mM imidazole and analyzed by SDS-PAGE.

Affinity purification of $Tom40_{HA}$

$Tom40_{HA}$ mitochondria were lysed with digitonin buffer containing 1% (w/v) digitonin. After removal of insoluble material, the supernatant was incubated with an anti-HA matrix (Roche) for 1-2 h at 4°C under constant shaking. Subsequently, the affinity matrix was washed with an excess amount of digitonin buffer containing 0.1% (w/v) digitonin. Bound proteins were eluted under denaturing conditions. For purification of bound Xdj1, ^{35}S-labeled Xdj1 was incubated with isolated $Tom40_{HA}$ mitochondria followed by affinity purification via anti-HA matrix.

Purification via Glutathione Sepharose

Similar amounts of recombinantly expressed and purified $_{GST}$Xdj1, $_{GST}$Djp1, $_{GST}$Ydj1 and GST were coupled in GST buffer (50 mM Tris/HCl, pH 7.5, 150 mM NaCl, 0.025% (v/v) Triton X-100) to Glutathione Sepharose 4B (GE Healthcare). To study binding of

mitochondrial proteins, mitochondria were lysed in digitonin buffer containing 1% (w/v) digitonin and the supernatant was incubated with Glutathione Sepharose 4B coated with GST alone or with GST-fused J-proteins. The binding was allowed for 2 h at 4°C under constant rotation. The affinity matrices were washed with an excess amount of GST buffer. Bound proteins were eluted with 10 mg/ml reduced glutathione in GST buffer. For *in vitro* protein-protein interaction studies recombinant $Tom22_{CD}$, $Tom70_{CD}$ or radiolabelled precursor proteins were incubated with Glutathione Sepharose 4B coated with GST alone or with GST-fused J-proteins in GST buffer for 1 h at 4°C under constant rotation. After excessive washing with GST buffer, bound proteins were eluted with 10 mg/ml reduced glutathione in GST buffer.

Precursor transfer assay

Radiolabelled Oxa1 precursor was incubated with Glutathione Sepharose 4B coupled with GST or $_{GST}$Xdj1 as described above. After excessive washing with GST buffer, the column material was incubated with recombinant amounts of the purified cytosolic domain of Tom22 in GST buffer containing 125 mM imidazole for 1 h at 4°C. For re-purification via His-tagged $Tom22_{CD}$, the elution sample was diluted in GST buffer and incubated with Ni-NTA agarose for 1 h at 4°C. Bound proteins were eluted with 500 mM imidazole in GST buffer. To study the import of Xdj1-precursor complexes, the Oxa1 precursor was incubated with $_{GST}$Xdj1 coupled to Glutathione Sepharose 4B as described above. After excessive washing, the Xdj1-bound Oxa1 precursor was eluted with 10 mg/ml reduced glutathione in GST buffer. The elution sample was diluted in import buffer and the *in vitro* import into isolated mitochondria was performed as described above.

Microscopy

The $Xdj1_{GFP}$ strain was grown at 30°C on selective medium lacking uracil and containing 3% (v/v) glycerol and 0.1% (w/v) glucose as carbon source. To stimulate expression of $Xdj1_{GFP}$ under control of the MET25 promoter, the cells were shifted to selective medium lacking methionine as well as uracil and containing 3% (v/v) glycerol for 3 h. The mitochondrial network was stained with MitoTracker Deep Red (Invitrogen) following the manufacturer's instructions. Wide field fluorescence microscopy was performed using an Olympus BX61 fluorescence microscope. UPLFLN 100x/1.3 objective (Olympus) and a F-view CCD camera (Soft imaging system) were used to acquire images. GFP fluorescence was visualized with a 470/40 nm bandpass excitation filter, a dichromatic mirror and 525/50 nm bandpass emission filter. MitoTracker Deep Red fluorescence was detected by a 562/40 nm bandpass excitation filter, a 593 nm dichromatic mirror and by a 624/40 nm bandpass filter. Z stacks images were made with an interval of 0.5 μm. Images were recorded using Cell-P software (Olympus).

Miscellaneous

The specificity of the antibodies used in this study was analyzed and confirmed by comparing isolated wild-type and corresponding mutant mitochondria or by using recombinant proteins. We used semi-dry western blotting to transfer the proteins from SDS- or blue native gels to PVDF membranes. Non-commercial enhanced chemiluminescence (ECL) was used for immunodetection (Ellenrieder et al., 2016). Signals were visualized on X-ray films (Amersham Hyperfilm ECL, GE Healthcare and Medix XBU, Foma) or by using the image reader LAS3000 (FujiFilm). MultiGauge software was used to quantify band intensities. X-ray films were scanned using ScanMaker 1000 XL and SilverFast XRay 6.6.2r1. ^{35}S-labeled proteins were detected by autoradiography using the Storm phosphorimager system (GE Healthcare). We removed non-relevant lanes digitally and indicated this by separating lines.

QUANTIFICATION AND STATISTICAL ANALYSIS

The software MaxQuant with its integrated search engine Andromeda (version 1.2.0.18) (Cox and Mann, 2008; Cox et al., 2011) was used for protein identification and SILAC-based quantification (Böttinger et al., 2015). Proteins were identified based on at least one unique peptide ($\geq$6 amino acids) and a false discovery rate of $<$ 1% applied to peptides and proteins. Protein quantification was based on unique peptides with at least one ratio count. The mean of $\log_{10}$-transformed $Tom22_{His}$/wild-type ratios was calculated ($n \geq 2$) and plotted against the corresponding p value determined using a one-sided Student's t test. A list of all proteins identified and quantified is provided in Table S1.

For quantifications of imported proteins or western blot signals, mean values with the corresponding standard error of the mean (SEM) are depicted as outlined in the figure legends. Mean values of three-five independent experiments were quantified. The exact number of replicates is provided in the figure and table legends. The MultiGauge software was used to quantify signal intensities of radiolabelled proteins and western blot signals.

DATA AND SOFTWARE AVAILABIITY

The mass spectrometry proteomics data have been deposited to the ProteomeXchange Consortium via the PRIDE partner repository with the dataset identifier PXD008203 (Vizcaíno et al., 2016).

Cell Reports, Volume *25*

Supplemental Information

Recruitment of Cytosolic J-Proteins by TOM Receptors Promotes Mitochondrial Protein Biogenesis

Łukasz Opaliński, Jiyao Song, Chantal Priesnitz, Lena-Sophie Wenz, Silke Oeljeklaus, Bettina Warscheid, Nikolaus Pfanner, and Thomas Becker

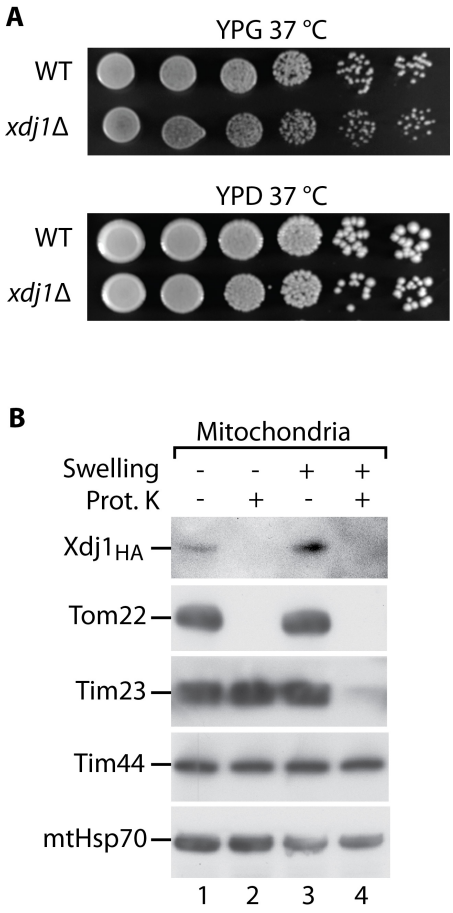

Figure S1. Growth of *xdj1*Δ Cells and Localization of Xdj1, Related to Figure 1

(A) Serial dilutions of wild-type (WT) and *xdj1*Δ cells were spotted on full medium containing a fermentable (glucose, YPD) or non-fermentable (glycerol, YPG) carbon source. Growth was analyzed at 37°C.

(B) Intact $Xdj1_{HA}$ mitochondria or osmotically swollen mitochondria (swelling) were treated with proteinase K (Prot. K) where indicated. Proteins were separated by SDS-PAGE and analyzed by immunodetection with the indicated antisera. $Xdj1_{HA}$ was detected with anti-HA antibodies.

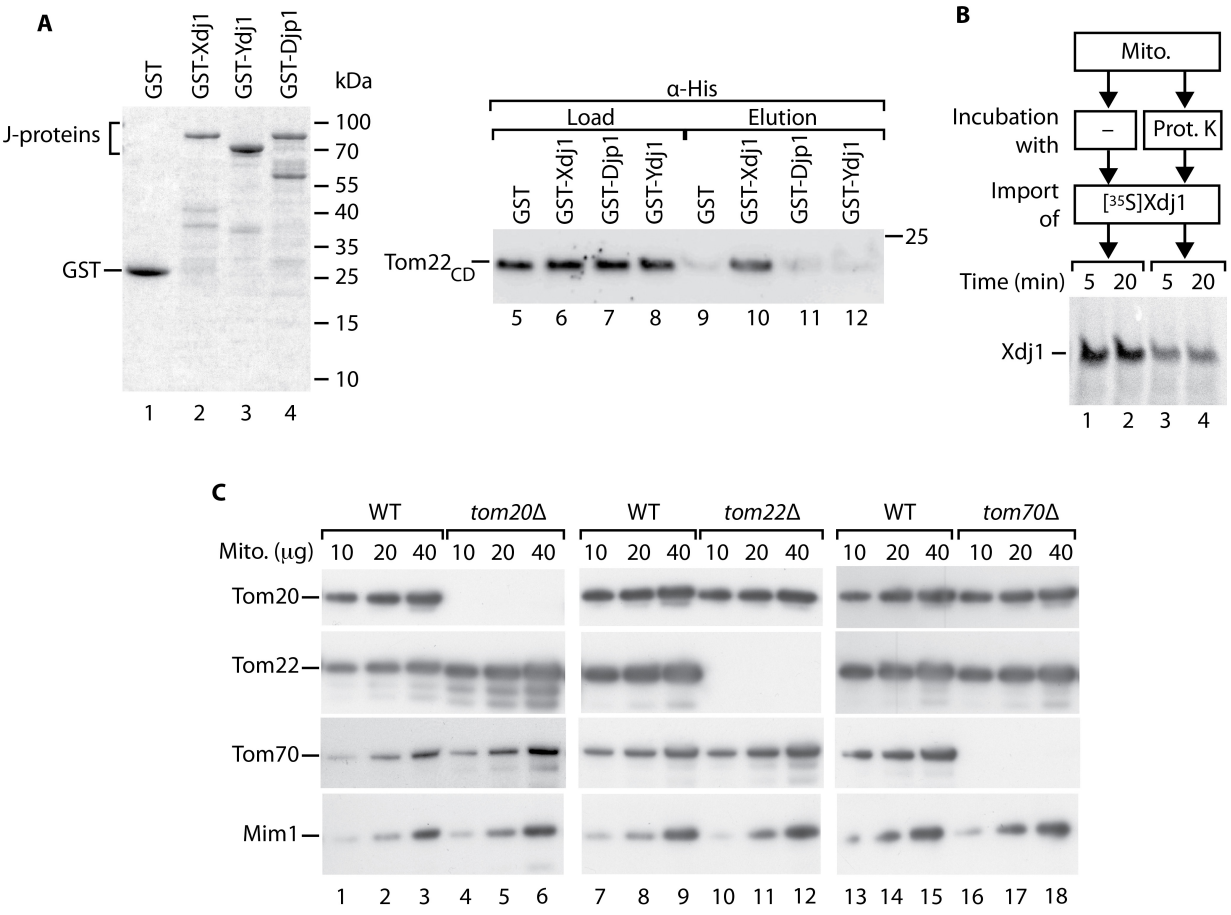

Figure S2. Analysis of Xdj1 Binding to Tom22 and Characterization of TOM Receptor Mutant Mitochondria, Related to Figure 1

(A) Left panel, the indicated recombinantly expressed and purified proteins were analyzed by SDS-PAGE and Coomassie blue staining. Right panel, the recombinantly expressed His-tagged cytosolic domain of Tom22 ($Tom22_{CD}$) was incubated with glutathione columns coated with GST, $_{GST}$Xdj1, $_{GST}$Djp1 or $_{GST}$Ydj1. Load and elution fractions were analyzed by SDS-PAGE and immunodetection with anti-His antibodies. Input for $Tom22_{CD}$ 2%; elution 100%.

(B) ^{35}S-labeled Xdj1 was incubated with isolated wild-type mitochondria. Where indicated, mitochondria were treated with proteinase K (Prot. K) before binding of [^{35}S]Xdj1.

(C) The indicated protein amounts of wild-type (WT), *tom20*Δ, *tom22*Δ and *tom70*Δ mitochondria were analyzed by SDS-PAGE and immunodetection with the indicated antisera. The lack of Tom20 leads to decreased levels of Tom22; the *tom20*Δ yeast strain used thus additionally contains a plasmid for expression of *TOM22*, leading to a moderate increase of Tom22 levels.

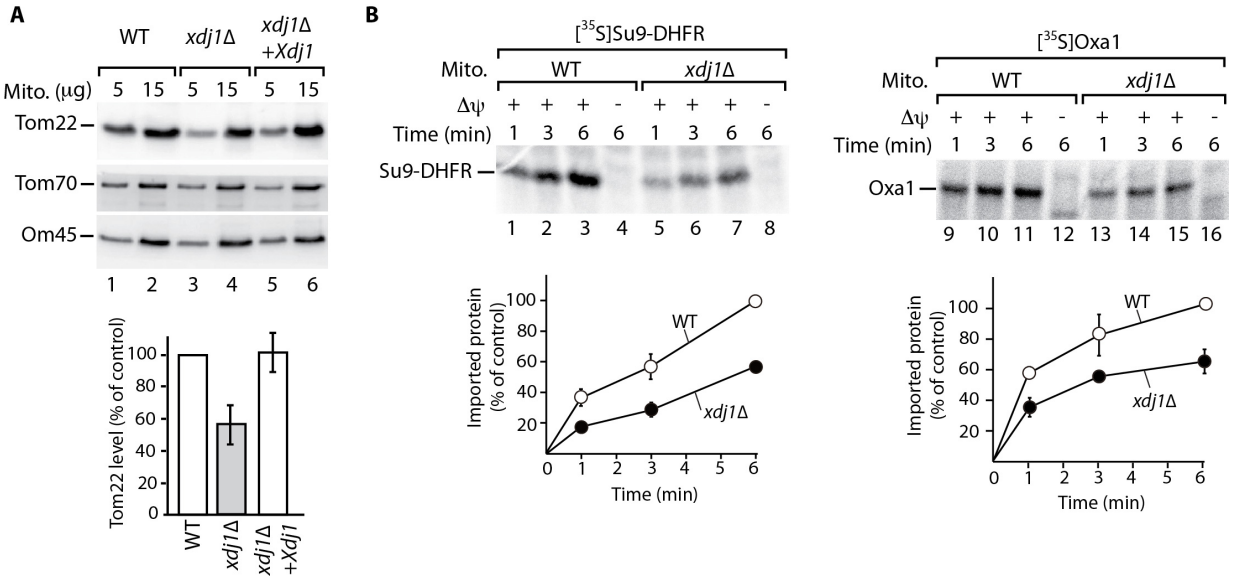

Figure S3. Characterization of *xdj1*Δ Strain and Mitochondria, Related to Figure 2

(A) Mitochondria from wild-type (WT), *xdj1*Δ and an *xdj1*Δ strain expressing plasmid-encoded *XDJ1* (*xdj1*Δ+*Xdj1*) were analyzed by SDS-PAGE and immunodetection. Quantification of Tom22 levels, depicted are mean values with standard error of the mean (n = 3). The amount of Tom22 in WT mitochondria was set to 100% (control).

(B) ^{35}S-labeled precursors of Su9-DHFR or Oxa1 were imported into WT and *xdj1*Δ mitochondria for the indicated periods. After import, non-imported precursor proteins were removed by treatment with proteinase K. The import reactions were analyzed by SDS-PAGE and autoradiography. Quantification of three independent import reactions with standard error of the mean. As control, the import of precursors into WT mitochondria after 6 min was set to 100%. Δψ, membrane potential.

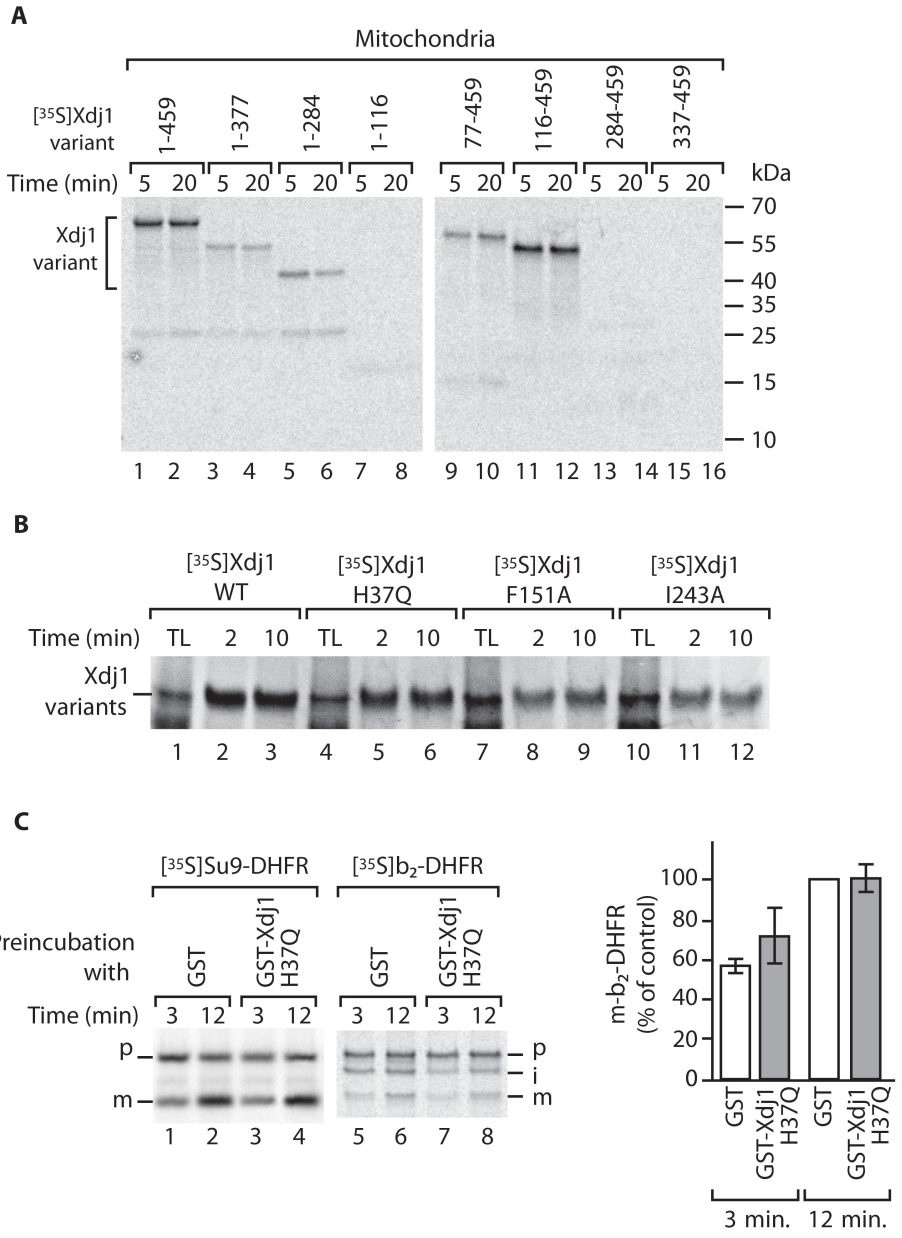

Figure S4. Analysis of Xdj1 Variants, Related to Figure 4

(A) ^{35}S-labeled Xdj1 constructs were incubated with isolated yeast wild-type (WT) mitochondria for the indicated periods. Mitochondria-bound proteins were analyzed by SDS-PAGE and autoradiography.

(B) ^{35}S-labeled Xdj1 variants were incubated with isolated WT mitochondria for the indicated periods. Mitochondria-bound proteins were analyzed by SDS-PAGE and autoradiography. TL, translation product, 14% of input.

(C) The precursors [^{35}S]Su9-DHFR and [^{35}S]b_2-DHFR were incubated with recombinantly expressed and purified GST, $_{GST}$Xdj1 or $_{GST}$Xdj1H37Q prior to import into isolated WT mitochondria. The import reaction was analyzed by SDS-PAGE and autoradiography. p, precursor; i, intermediate; m, mature. Quantification of mature-sized [^{35}S]b_2-DHFR, mean values with range (n = 2); the import after 12 min in the presence of GST was set to 100% (control).

Table S1. List of Proteins Identified in $Tom22_{His}$ Affinity Purification Experiments, Related to Figure 1

Identification of proteins purified with $Tom22_{His}$ and SILAC-based relative quantification were performed using MaxQuant/Andromeda (version 1.2.0.18). Potential Tom22 interaction partners were defined as proteins with an enrichment factor of > 10, an overall sequence coverage of ≥ 4%, and a p-value of < 0.05. See Excel file for results.

Table S2. Oligonucleotides Used in This Study, Related to STAR Methods

Name	Sequence (5'->3')	Source	Identifier
pGEX-XDJ1for	CGGGATCCCGATGAGTGGCAGTGATAGAGG	This paper	1996
pGEX-XDJ1rev	TCCCCCCGGGGGGATCATTGGATACAGCAGTACGAAC	This paper	1997
pGEX-YDJ1for	CGGGATCCCGATGGTTAAAGAAACTAAGTTTTACGATATTC	This paper	1998
pGEX-YDJ1rev	TCCCCCCGGGGGGATCATTGAGATGCACATTGAACAC	This paper	1999
pGEX-DJP1for	CGGGATCCCGATGGTTGTTGATACTGAGTATTACG	This paper	2000
pGEX-DJP1rev	TCCCCCCGGGGGGATCATGTATGTCTCTTCTTTTTTGTAGC	This paper	2001
XDJ1H37Qfor	GCTTACAGAAAGCTTGCCCTGAAACATCAACCGGACAAGTATGTGGATCAAGACTCA	This paper	2002
XDJ1H37Qrev	TGAGTCTTGATCCACATACTTGTCCGGTTGATGTTTCAGGGCAAGCTTTCTGTAAGC	This paper	2003
XDJ1-HAfor	AGCGCATCAGAAAGCAAGAAGTTCGTACTGCTGTATCCAACGGATCCCCGGGTTAATTAA	This paper	2004
Xdj1-HArev	GAAAAAAAAAAAAAAATAGAATAAAAAGTTATTGATGCCAGAATTCGAGCTCGTTTAAAC	This paper	2005
SP6-XDJ1for	TCGATTTAGGTGACACTATAGAATACGCCGCCGCCATGAGTGGCAGTGATAGAGGAG	This paper	1326
SP6-XDJ1Rev	GATCTCATTGGATACAGCAGTACGAAC	This paper	1327
SP6-OXA1for	TCGATTTAGGTGACACTATAGAATACGCCGCCGCCATGTTCAAACTCACCTCTCGAC	This paper	1334
SP6-OXA1rev	GATCTCATTTTTTGTTATTAATGAAGTTTG	This paper	1335
SP6-TOM22for	TCGATTTAGGTGACACTATAGAATACGCCGCCGCCATGGTCGAATTAACTGAAATTAAAGACG	This paper	1322
SP6-TOM22rev	GATCTTAATTGGCTGTTGCTGCAG	This paper	1323
CCXDJ1-GFPfor	ATATCTAGAATGAGTGGCAGTGATAGAGGAG	This paper	2006
CCXDJ1-gfprev	TTGTCGACTTGGATACAGCAGTACGAACTTC	This paper	2007
SP6-XDJ177-458for	TCGATTTAGGTGACACTATAGAATACGCCGCCGCCATGGGTGATGATAATGGTGCCGCT	This paper	2008

SP6-XDJ 116-458for	TCGATTTAGGTGACACTATAGAATACGCCGCC GCCATGGGCGAGTATGATGCGTACGAA	This paper	2009
SP6-XDJ 284-458for	TCGATTTAGGTGACACTATAGAATACGCCGCC GCCATGGAAAACTTGGAGCAGAAGCAA	This paper	2010
SP6-XDJ 377-458for	TCGATTTAGGTGACACTATAGAATACGCCGCC GCCATGCCACCAGATAACTGGTTCAAT	This paper	2011
SP6-XDJ 1-377rev	GATCTCATGGAAATTCAATATGAACGAA	This paper	2012
SP6-XDJ 1-284rev	GATCTCATTCTTGTTTTTCAGTGAGATG	This paper	2013
SP6-XDJ 1-116rev	GATCTCAGCCAGGGAAATTATTTCCATC	This paper	2014
XDJ1WG for	CTTTAAGAAGGAGATATACCATGAGTGGCAGT GATAGA	This paper	2015
XDJ1WG rev	TGATGATGAGAACCCCCCCCTTGGATACAGC AGTACGA	This paper	2016
pRS416-XDJ1for	AGGGGAATTCAAACTCGTTATTCGAAGTTTTC	This paper	1990
pRS416-XDJ1rev	AGGGGGATCCGTAGTGTTTTTGGAAGAGATG C	This paper	1991
XDJ1-F151Afor	ATGGGCAAGAAGCTGAAGGCTGATTTAAAGA GACAGGTC	This paper	1992
XDJ1-F151Arev	GACCTGTCTCTTTAAATCAGCCTTCAGCTTCT TGCCCATG	This paper	1993
XDJ1-I243Afor	CTGTCAAAGAAGGAAATCGCTACAGTGAACG TGGCTCCG	This paper	1994
XDJ1-I243Arev	CGGAGCCACGTTCACTGTAGCGATTTCCTTCT TTGACAG	This paper	1995